Agulhas, collectively administered by SANAP (the South African National Antarctic Programme). SANAP in turn is a subdirectorate of South Africa's Department of Environmental Affairs and Tourism (DEAT).

Every 12 months the SANAP stations in Antarctica (i.e. SANAE IV and E-Base) are visited during what is referred to as the summer takeover period. Fresh food, diesel fuel, a temporary maintenance crew and a new overwintering team are transported to the station. SANAE IV comfortably houses the entire takeover crew, which may number up to 80 people, yet only the overwintering team, totalling approximately 10 people, will remain behind after the takeover is complete. The station is constructed from three main blocks (viz. the A-, B- and C-Blocks) and two smaller interconnecting passages or "links", with the laboratories, living-quarters and heavy machinery distributed in the A, B and C sections respectively. Notably, SANAE IV is a South African design and construction (completed in 1997).

Figure 1.4: South Africa's SANAE IV station, completed in 1997 (Olivier, 2005)

1.2 Objectives

The efforts required to operate SANAE IV and other SANAP stations are intensive. Thus, in view of the associated costs of running South Africa's Antarctic stations as well as an increasing global awareness of alternative energy-generation methods this study aims to investigate the feasibility, and sensibility, of harnessing solar energy incident at SANAE IV.

Utilising solar energy in Antarctica is not a novel idea. America, Australia, Japan, Spain and Sweden have all commissioned solar energy systems at their stations, while Australia, Germany and Sweden are further investigating the possibility of installing hybrid solar- and wind-powered hydrogen fuel-cell systems. Teetz (2002) has already investigated the feasibility of installing a

wind turbine at SANAE IV and concluded that it would be advantageous to do so, although to date no device has yet been installed at the station. The American, Argentinean, Australian, German, Indian, Japanese, Spanish and Swedish stations on the other hand are all currently utilising wind energy. In fact, the Australian Mawson base has achieved the target of generating an unprecedented 80 % of its energy demand from wind power.

Such efforts by countries to install renewable energy systems at their Antarctic stations are strongly encouraged by the Antarctic Treaty. For instance, in 1991 during the XIth Antarctic Treaty Special Consultative Meeting (ATSCM) a noteworthy decision was made to adopt the Madrid Protocol (Madrid Protocol, 1991) to the Antarctic Treaty. Essentially this protocol states that signatories to the Treaty are *"…convinced of the need to enhance the protection of the Antarctic environment and dependent and associated ecosystems"*. Furthermore it is stated in the Protocol that, *"The Parties commit themselves to the comprehensive protection of the Antarctic environment and dependent and associated ecosystems and hereby designate Antarctica as a natural reserve, devoted to peace and science."* As a result it was established during the XIth ATSCM that *"…the use of alternative energies, such as solar and wind power in the Antarctic Treaty Area, and the study of a systematic way of implementing energy saving methods with the aim of reducing the use of fuels to the maximum extent possible* [should be investigated]*"* (Steel, 1993). This project aims to proceed with the mandate issued at the XIth ATSCM, and to determine the potential benefits that might arise from the suggested changes to SANAP operations in Antarctica.

Figure 1.5: Where the Antarctic ice-shelf, suspended in the ocean, breaks off into icebergs

(Olivier, 2005)

1.3 Layout of Thesis

This thesis has been divided into six chapters. Chapters 2-4 essentially pose questions intended to assist in determining the feasibility of utilising solar energy at SANAE IV. These questions address: the amount of incident solar radiation at SANAE IV, the amount of energy consumed by the station, a consideration of what one could use to capture solar energy at SANAE IV, and an evaluation of expected lifecycle costs. The information obtained from each of these sections was collated, and an answer on the technical and economic feasibility of utilising solar energy at South Africa's Antarctic station and the recommended course of action are provided in the final chapter (Chapter 6).

To summarise, this thesis contains the following six chapters:

- Chapter 1 – Background
- Chapter 2 – Available Solar Energy at SANAE IV in Antarctica
- Chapter 3 – SANAE IV Energy Demand
- Chapter 4 – Solar Energy Capturing Solutions
- Chapter 5 – Economic Analysis
- Chapter 6 – Conclusion

The investigation described in chapter 2 has been limited by the size of a relatively small set of actual measured data obtainable from SANAE IV. Nonetheless, suggested values are well supported by an examination of three alternative resources and accuracy estimates have been made. Predicted values of radiation at various tilt angles are also presented. The end of the chapter includes a comparison of the expected radiation at SANAE IV with data from three other Antarctic stations (viz. the Dumont d'Urville [FRA], WASA [SWE] and Neumeyer [GER] bases).

Chapter 3 includes a review of work previously undertaken at SANAE IV by Cencelli (2002) and Teetz (2002). It is considered important for understanding how much energy is consumed at the station. Energy loads found suitable for utilising solar energy are identified and observations regarding potential efficiency improvements at the station are made. It is also shown how the entire energy system of SANAE IV can be divided into an electrical and a thermal energy demand, the same two categories that define solar energy systems.

Chapter 4 investigates the alternative methods of capturing solar energy, and describes which of these are optimal for the conditions at SANAE IV. Some of the difficulties encountered due to the low ambient temperatures and strong winds are highlighted, and the expected collector efficiencies of various available products are calculated. Each of the recommended solutions has been described in terms of its expected energy savings, as well as by way of examining the associated prices of each product.

Chapter 5 presents an economic analysis based on the *"Integrated Environmental Management Information Series"* published for the Department of Environmental Affairs and Tourism (DEAT, 2005). Payback periods, energy generation costs and externalities are calculated and then discussed.

Finally, conclusions are given in chapter 6. Here an answer is given regarding the feasibility of utilising solar energy at South Africa's SANAE IV station in Antarctica. Included are recommendations and the suggested future course of action.

Figure 1.6: Joint German and South African logistics on the ice-shelf (Olivier, 2005)

Chapter 2 – Available Solar Energy at SANAE IV in Antarctica

2.1 Introduction

Investigating the feasibility of using solar energy at South Africa's SANAE IV base in Antarctica necessitates a careful study of the insolation received throughout the year. This chapter aims to provide an answer to the question of how much solar energy is available for the displacement of diesel at the base and under what conditions this insolation will be available.

Section 2.2 of this chapter endeavours to provide a first approximation of the expected average insolation rates at SANAE IV. To this end the databases maintained by the National Aeronautic and Space Agency (NASA) have been investigated for the locations of the South African (SANAE IV) and German (Neumeyer) stations located approximately 300 km from each other. These databases, created using satellite imagery and ground-based measurements from around the world, currently represent the most modern method of mapping meteorological information on a global scale. The section therefore also aids in understanding how solar radiation conditions at SANAE IV compare to other locations around the world.

Next a theoretical analysis of solar radiation at SANAE IV is presented. Here various correlations are investigated and compared with the values suggested by NASA, helping to further establish what the most probable amounts of radiation at the South African station are. A small amount of data measured at SANAE IV during 2005 is also analysed in these comparisons and the results from correlations that most adequately describe the radiation conditions in Antarctica are identified. Subsequently these results are used to estimate the performance of solar energy devices in chapters 4 and 5.

Finally, a short summary of the investigation and some conclusions are provided. Accuracy estimates are presented and the areas that would most benefit from future study are highlighted.

8

2.2 Global Databases – A First Estimate

The NASA database utilised in this section was established in 1986 after competition amongst various international agencies resulted in an effort to collate measurements of solar radiation from around the world. Ultimately NASA became the benefactor of this information and has made it available in the Surface Radiation Budget (SRB) and Surface meteorology and Solar Energy (SSE) datasets (SSE, 2005).

Figure 2.1 is compiled with data from NASA's SSE dataset and illustrates estimates of annual average insolation everywhere on Earth for flat surfaces (i.e. horizontal insolation). According to this image (which accounts for local weather, or *all-sky* conditions) the high latitudes receive less global horizontal insolation on average over a year than the more central equatorial regions, due mainly to the *cosine effect* or low average zenith angle at high latitudes.
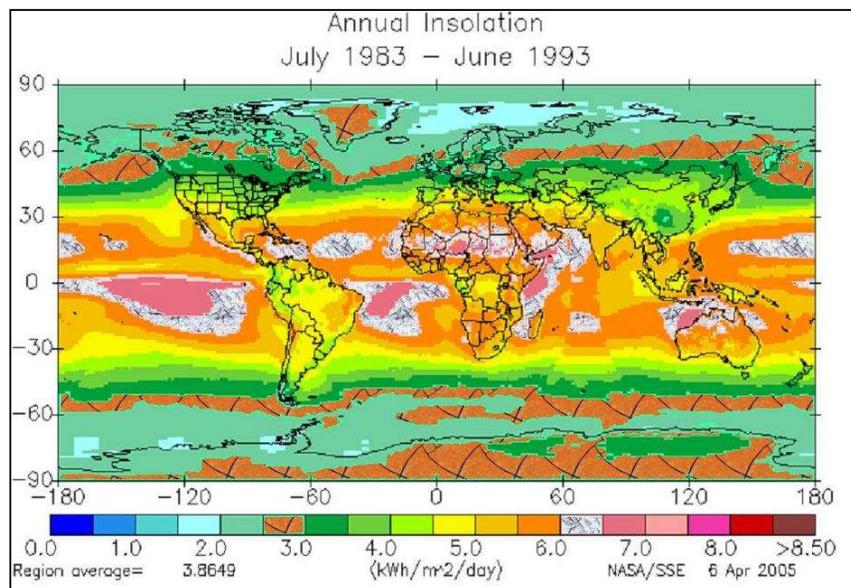

Figure 2.1: Estimated average total all-sky global horizontal insolation (SSE, 2005)

It is possible, however, to tilt collector surfaces at higher latitudes towards the sun and mitigate the disadvantages of the obliquely received sunlight. In fact, calculating the annual insolation on two-axis tracking surfaces reveals that every location on the planet would, not considering the effect of the Earth's atmosphere, receive equal amounts of energy from the sun. Consequently two significant criteria in the current investigation are the added cost of installing tracking mechanisms, and the local weather conditions at SANAE IV. Unfortunately, latitude also has

9

bearing on the received insolation for another reason. Even on clear days there are absorptive and reflective losses of radiation associated with the distance sunlight travels through the atmosphere, which is a maximum at the poles. This effect is summarised in a parameter referred to as *air-mass.*

Therefore, as shown in figure 2.1 it is evident that the more central and sun facing equatorial latitudes are better disposed to harnessing solar energy than the polar-regions. There is less need for tracking surfaces, a lower air-mass and not as much seasonal variation of radiation. According to figure 2.1 these latitudes receive on average approximately 3 kWh/m^2, or 200 % more horizontal radiation than Antarctica and other polar-regions annually.

Figure 2.2 illustrates the southern-hemisphere summer radiation conditions. Antarctica receives very high insolation during the summer mainly because the sun remains above the horizon throughout the day. Even when considering all-sky conditions it is evident that Antarctica has extremely high flat-plate insolation rates during this short period. In fact, together with western parts of Australia and South Africa's Northern Cape, they are the highest in the world during the southern-hemisphere summer months.
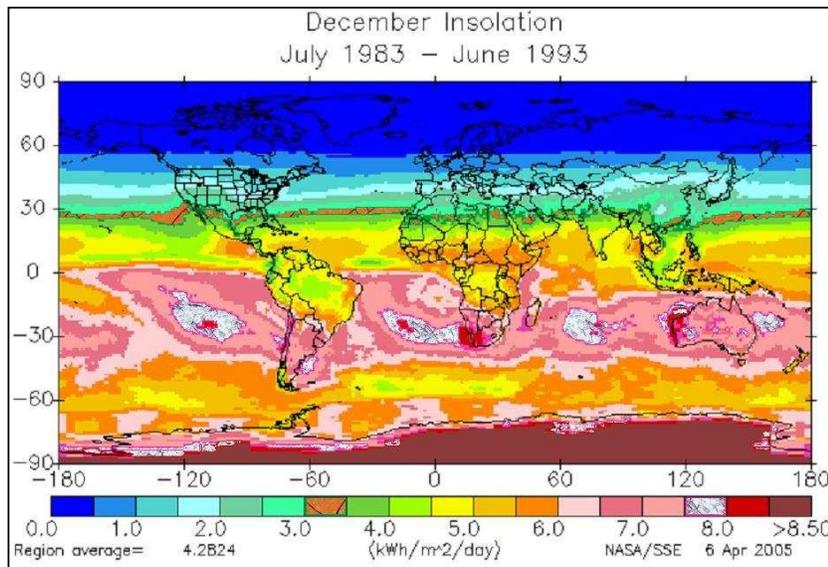

Figure 2.2: Estimated average December total horizontal insolation (SSE, 2005)

A plot of the estimated daily-total horizontal insolation (in kWh/m^2) incident at SANAE IV over the five-year period from 1988 until 1992 is given in figure 2.3. From the figure it is evident that surface insolation is a maximum from late November to early January (coincident with the summer solstice on the 21st of December), and that minima are encountered during winter when

zero sunlight is present. It can be seen that Top Of Atmosphere (TOA) radiation remains constant throughout annual cycles, and it is estimated from figure 2.3 that on a clear summer's day 9 kWh/m^2 of insolation should be received at ground level.
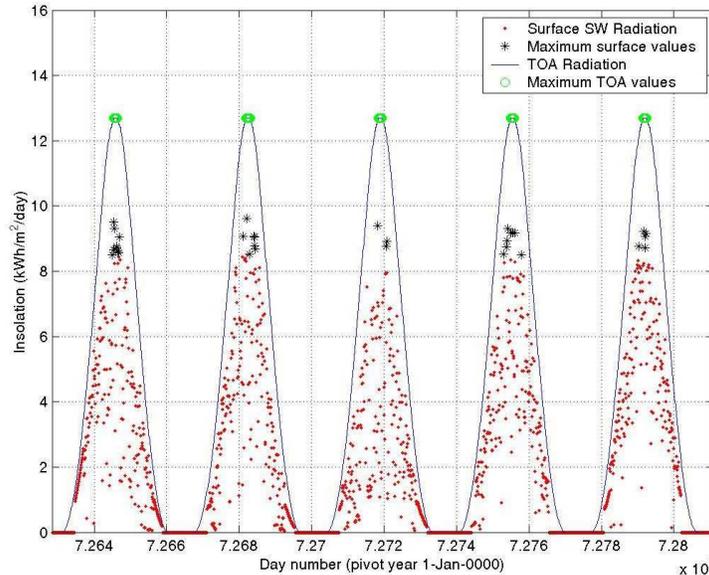

Figure 2.3: Surface and TOA horizontal insolation at SANAE IV, 1988 to 1992 (SSE, 2005)

Also derived from the SSE database is figure 2.4. Here the annual average radiation at SANAE IV is shown in greater detail and it can be seen, for instance, that during December at noon approximately 650 W of radiation will fall on a horizontal surface. A more detailed investigation of the solar radiation expected at SANAE IV, which studies the theory of clear-sky and all-sky conditions, follows in section 2.3.
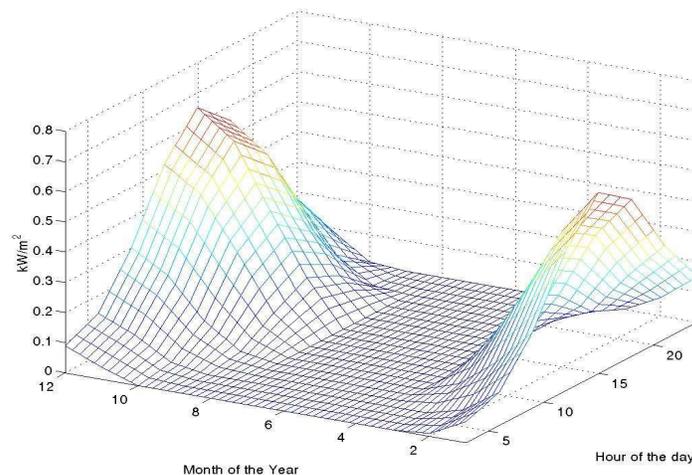

Figure 2.4: Monthly-average daily global horizontal radiation at SANAE IV (SSE, 2005)

2.3 Solar Radiation at SANAE IV – A Theoretical Study

2.3.1 Data Capture Instrumentation and Procedures

All references in this thesis to measurements of radiation recorded at SANAE IV pertain to data obtained by the author during the 2004/2005 takeover. Instrumentation used included: one Kipp & Zonen SP-*Light* pyranometer, two Kipp & Zonen CM5 pyranometers, a Hewlett-Packard 34970A data logger, shielded low-temperature resistant cable, a 5-Watt Liselo-Solar photovoltaic (PV) module, thermocouples, and a shade-ring that was designed by the author and manufactured locally. Measurements were recorded to a personal computer each second for eighteen days (10th till 27th January 2005), however the data presented here are one-minute averages of the original set. The photovoltaic (PV) module was used to determine PV energy output and cell temperatures, and simultaneous temperature measurements of all instrumentation were taken using the thermocouples which enabled corrections to be made for thermal effects.

2.3.2 Clear-Sky Radiation

Clear-sky correlations model the surface radiation conditions without considering the influence of clouds. Of these Hottel (1967) has presented a method for estimating the clear-sky global radiation that accounts for four different climate types, and Liu and Jordan (1960) have presented methods for estimating global clear-sky diffuse radiation from these values. Figure 2.5 utilises these correlations to plot curves of the January global clear-sky horizontal and diffuse radiation alongside data measured at SANAE IV (the details of which are given in section 2.3.1). Also plotted in figure 2.5 for comparison are the ASHRAE standard atmosphere (an average atmosphere for every location on Earth) and a Hottel curve with coefficients that have been adjusted in order to replicate measured data more accurately (the details of which are given at the end of section 2.3.2).

From figure 2.5 it is evident that all of the unadjusted correlations underestimate the global radiation at SANAE IV. This underestimation has been attributed to the relatively clear skies of Antarctica since the suggested equations are measured averages that account for the haziness of other sites. From figure 2.5 it has also been calculated that on a clear-sky day in January at SANAE IV a total of 9.1 kWh will be available per square metre of horizontal surface. That is, 379 W/m^2 for a 24-hour period. The diffuse radiation plotted in figure 2.5 is predicted acceptably

well by Liu and Jordan (1960) and is the suggested correlation for future use, however, it is not advisable to use the simple ASHRAE standard atmosphere model.
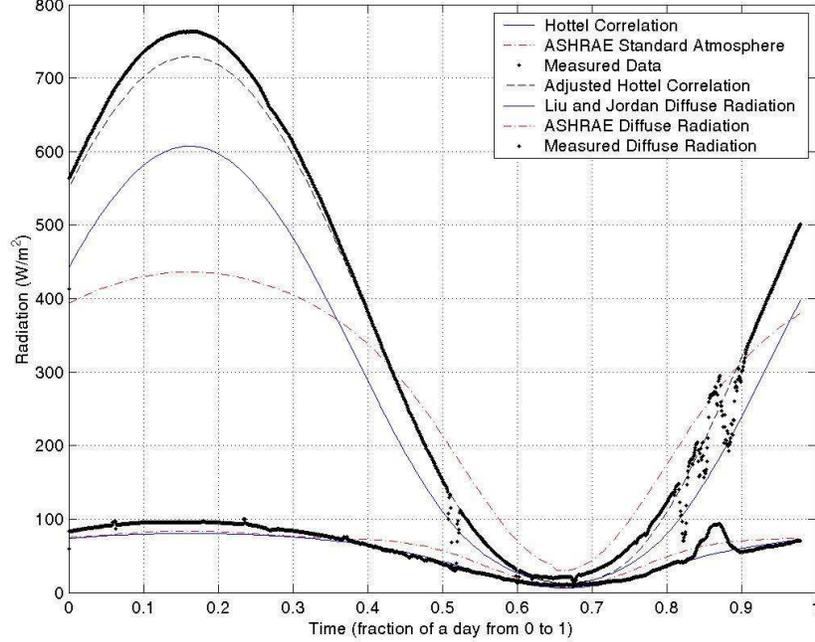

Figure 2.5: Clear-sky curves of daily radiation at SANAE IV

Both the Hottel and the Liu and Jordan correlations mentioned above (which were used to predict clear-sky global radiation and clear-sky diffuse radiation respectively) are presented below. Here the subscripts *"cnb"* refer to clear-sky normal beam radiation, *"on"* to TOA normal beam radiation and *"b"* to beam radiation. The effect of clear-sky atmospheric effects can then be approximated by:

$$G_{cnb} = G_{on} \cdot \tau_b \qquad\qquad 2.1$$

Where G_{on} (W/m^2) in equation 2.1 is easily calculated from equations provided by Duffie and Beckman (1991), and τ represents the atmospheric transmissivity at SANAE IV suggested by Hottel (1967). If *Al* is the altitude of the location in kilometres, τ is approximated as:

$$\tau_b = a_0 + a_1 \cdot e^{\left(\frac{-k}{\cos\theta_z} \right)} \qquad\qquad 2.2$$

Where,

$$a_0 = r_0 \cdot a_0' \qquad a_0' = 0.4237 - 0.00821 \cdot (6 - Al)^2$$

$$a_1 = r_1 \cdot a_1' \qquad a_1' = 0.5055 + 0.00595 \cdot (6.5 - Al)^2$$

$$k = r_k \cdot k' \qquad k' = 0.2711 + 0.01858 \cdot (2.5 - Al)^2$$

Table 2.1: Hottel climate coefficients

CLIMATE TYPE	r_0	r_1	r_k
Tropical	0.95	0.98	1.02
Midlatitude summer	0.97	0.99	1.02
Subarctic summer	0.99	0.99	1.01
Midlatitude winter	1.03	1.01	1.00

From Hottel (1976)

The fitted or adjusted Hottel curve shown in figure 2.5 uses:

$$r_0 = 0.99 \qquad\qquad r_1 = 0.99 \qquad\qquad r_k = 0.45$$

The correlation proposed by Liu and Jordan for estimating the amount of diffuse radiation is:

$$\tau_d = \frac{G_d}{G_o} \qquad \text{Where,} \qquad \tau_d = 0.271 - 0.294 \cdot \tau_b \qquad\qquad\qquad 2.3$$

2.3.3 All-Sky Conditions

The interaction of clouds with incoming solar radiation makes it very difficult to accurately predict the actual surface insolation throughout the year. *All-sky* correlations must surpass modelling only the effects of water vapour, ozone and particulate matter in the atmosphere (i.e. transmissivity), and for this reason are normally derived empirically. To predict actual values of surface insolation analytically is very difficult, and in fact Norris (1968) concludes that, *"The foregoing discussion… indicate*[s]*… it is probably impossible to use cloud information to predict solar radiation."* Therefore, since recorded data will automatically reflect the effect of cloud conditions specific to a location and provide acceptable averages for further investigation, there is little that can replace a database of previously measured radiation.

Unfortunately values of solar insolation are not currently being recorded at SANAE IV even though the base is classified as a first class weather station. Thus, instead of seeking correlations

that relate cloud cover data (available at SANAE IV) to insolation, a number of methods collated by Duffie and Beckman (1991) will form the basis of further investigation.

HORIZONTAL SURFACES – ANALYSIS FOR JANUARY

An important parameter used often in the correlations presented by Duffie and Beckman (1991) is the *clearness index*, and is simply the ratio of global horizontal radiation on the Earth's surface to that at the TOA. TOA insolation is easily calculated for any location on Earth, and global horizontal radiation is a standard measurement that forms part of any solar radiation dataset. Thus, knowing the global horizontal insolation the clearness index can easily be derived from:

$$\overline{K}_T = \frac{\overline{H}}{\overline{H}_O} \hspace{8cm} 2.4$$

Where $\overline{K}_T$ is the monthly average clearness index (dimensionless), $\overline{H}$ is the monthly average daily radiation on a horizontal surface (kWh/m^2) and $\overline{H}_O$ is the monthly average daily TOA radiation on a horizontal surface (kWh/m^2). There are also analogous equations for daily and hourly clearness indices defined by K_T and k_T respectively.

From clearness indices Erbs et al. (1982) have suggested a well-known and widely used method to predict the values of *diffuse* radiation. The correlation was created using data from one Australian and four American weather stations, yet referring to figure 2.6 (Neumeyer, 2005), it can be seen that this method underestimates the amount of diffuse radiation for conditions in Antarctica. The recorded data shown in figure 2.6 was measured at Neumeyer by instrumentation endorsed by the Baseline Surface Radiation Network (BSRN), of which the German base is a member. This is a significant observation since concentrating solar energy systems utilise only the beam portion of incoming solar radiation, and consequently the correlations suggested by Erbs et al. (1982) are regarded as inappropriate for further investigation at SANAE IV.
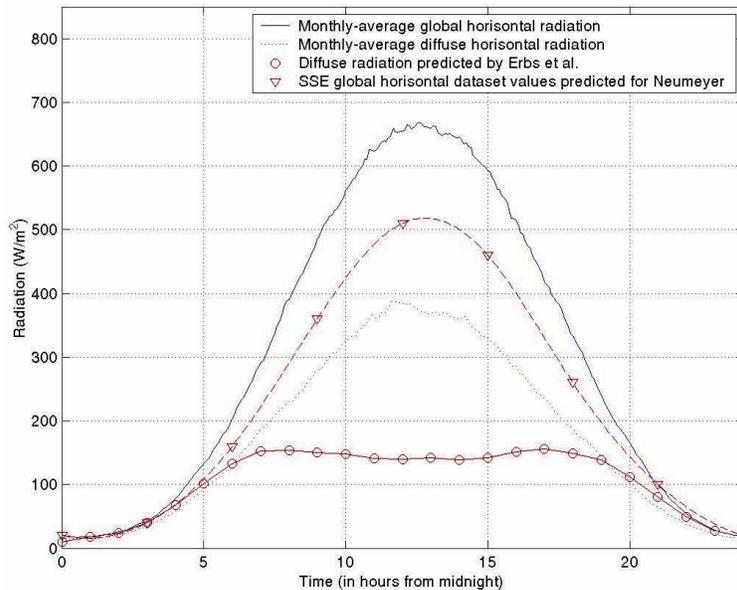
Figure 2.6: Five-year average January daily radiation at Neumeyer station (1994 to 1998)

From figure 2.6 it is also evident that SSE values tend to underestimate the global horizontal radiation for locations in Antarctica. The underestimation has been calculated as 24 % of the daily peak value and just over 20 % of the total daily horizontal insolation. Yearly weather conditions, however, may vary by this much (SSE suggests seasonal average variations of 17 % in January), thus it can be said that for the location of Neumeyer the SSE database presents useful estimates of worst-case conditions.

SSE also provides estimates of average cloud cover, and a quick consideration of other available meteorological data is in order. Cloud cover observations taken at Neumeyer station suggest an average January cloud cover of 7/10ths (or 70 %), and compares well to the amount given in SSE of 67.6 %. Comparatively, visual observations recorded at SANAE IV suggest a cloud cover of 4/10ths at the South African station while the value presented by NASA's database is 51.7 %. It is reasonable, therefore, to assume that SANAE IV is expected to experience less cloud cover than Neumeyer during January. The direct implication of this is that SANAE IV will also experience higher values of global horizontal radiation and lower relative amounts of diffuse radiation than Neumeyer.

Note that although reference was made earlier to the statement by Norris (1968) that, *"The foregoing discussion… indicate*[s]*… it is probably impossible to use cloud information to predict solar radiation"* this does not imply that higher amounts of cloud cover are not analogous with

16

lower amounts of global radiation for adjacent locations. Rather, it only states that one cannot conclude by exactly how much the levels of radiation at these locations will differ.

The most accurate averages of expected insolation are still derived from recorded data however, and in figure 2.7 measurements of radiation logged at SANAE IV over an eighteen-day period during January 2005 (10th till 27th January 2005) are presented (as specified in section 2.3.1). The average clearness index of the period is 51.2 % (refer to equation 2.4), and plotted alongside is SSE global radiation data. Considering that the five-year clearness index of Neumeyer is 63.7 % (from the data in figure 2.6) and is a location known to have higher amounts of cloud cover than SANAE IV, it is evident that the data presented in figure 2.7 represents a particularly cloudy January period. It is again apparent that SSE values are conservative approximations of the actual conditions in Antarctica.
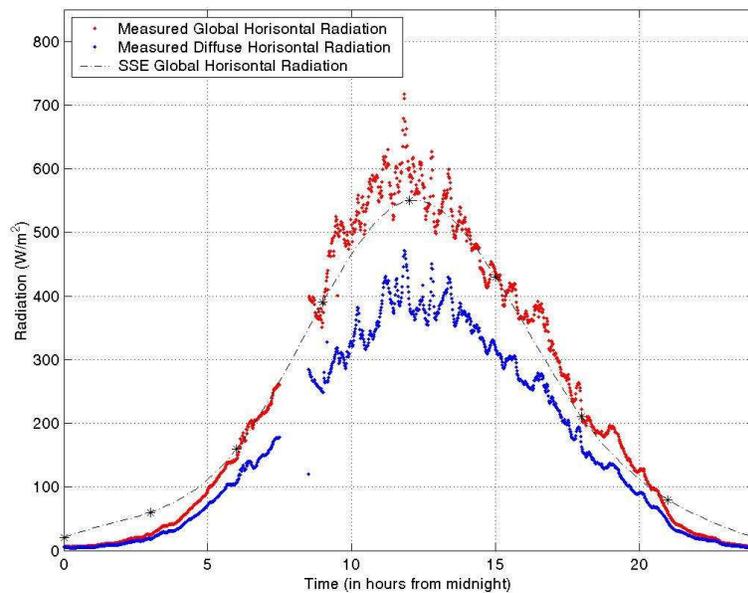

Figure 2.7: Comparison of SANAE IV data with values predicted by the SSE dataset

The suggested equations for calculating the January radiation at SANAE IV are presented in equations 2.5 and 2.6. They were created by incrementing SSE dataset values by 20 %, and are essentially equal to the average radiation conditions at Neumeyer (refer to figure 2.12). As stated above this is known to be a conservative estimate. The diffuse radiation was calculated by determining the relative fraction of diffuse to global radiation at Neumeyer, and applying this condition to the global radiation at SANAE IV. For a list of the equations pertaining to other months please turn to appendix B.1.

Monthly-average instantaneous global horizontal radiation (W/m^2) where x is a number in hours from 0 to 24 is given by equation 2.5.

$$G = -0.0003187x^6 + 0.024072x^5 - 0.64063x^4 + 6.8013x^3 - 22.662x^2 + 33.863x + 6.5175 \qquad 2.5$$

Monthly-average instantaneous diffuse horizontal radiation (W/m^2) where x is a number in hours from 0 to 24 is given by equation 2.6.

$$G_d = -0.0001608x^6 + 0.012169x^5 - 0.32434x^4 + 3.4278x^3 - 11.02x^2 + 16.759x + 11.998 \qquad 2.6$$

Table 2.2: Estimated January radiation averages for the conditions at SANAE IV

PARAMETER	VALUE
January-average global horizontal insolation (kWh/m^2)	7.3
January-average midday global horizontal radiation (W/m^2)	663
January-average mean global horizontal radiation over 24 hours (W/m^2)	304

THE EFFECT OF SURFACE TILT

The importance of surface tilt was alluded to earlier in section 2 of this chapter where it was noted that valuable gains may be realised by proper management of the *cosine effect*. Analysing these gains, however, poses certain problems. Although tilting a collecting surface towards the sun will increase the beam radiation in a manner simply proportional to the cosine of the zenith angle, the diffuse radiation changes independently according to the tilt angle, reflectivity of the ground and view factor with the sky. Consequently it is necessary to know both the diffuse and beam radiation before it is possible to determine available tilted insolation.
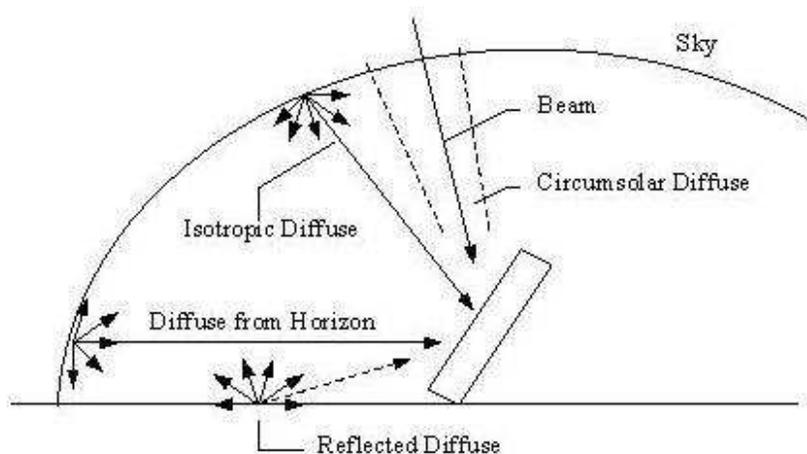

Figure 2.8: Components of beam and diffuse radiation (Duffie et al., 1991)

18

A further complication is the modelling of the individual responses to tilt of various components of diffuse radiation (refer to figure 2.8). Included are the components of horizon brightening (a band of higher intensity diffuse radiation at the horizon), circumsolar radiation (high intensity diffuse radiation in the vicinity of the sun), isotropic, and reflected ground components. For the purposes of this study it will be assumed that the diffuse reflective surface of snow reflects 70 % of the incident radiation (Duffie and Beckman, 1991), although Schmidt et al. (1994) have suggested a value of 84 %.

Determining global tilted radiation allows the use of any or all of the above-mentioned factors, depending on the accuracy desired. Perez et al. (1988) have considered all of these factors in their correlation (the utilisation of which has led to the creation of figures 2.9 and 2.10) while Liu and Jordan (1963) assume that the intensity of diffuse radiation is equal at any orientation. These two approximations, which will be referred to again, are known as the anisotropic and isotropic conditions respectively.
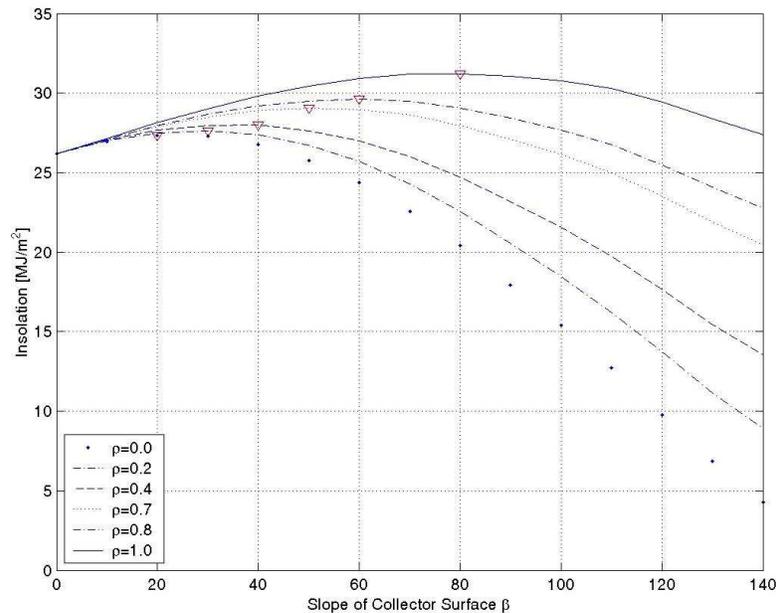

Figure 2.9: January daily insolation rates on a tilted surface with different ground reflectivity

From studying figure 2.9 (refer to appendix B.2 for computational details) it is evident that the optimum tilt angle for global radiation at SANAE IV during January is 52° from the horizontal. At this angle an increase of 11 % in daily insolation is expected.

Available beam radiation at various tilt angles is shown in figure 2.10. In this instance ground reflectivity is of no significance since beam radiation reflected from the snow is scattered diffusely, and there exists only a single curve as opposed to the various lines visible in figure 2.9. The optimum tilt for a collector that utilises only beam radiation is 39°, and is associated with a 21 % increase in incident radiation compared to the insolation received on a horizontal surface.
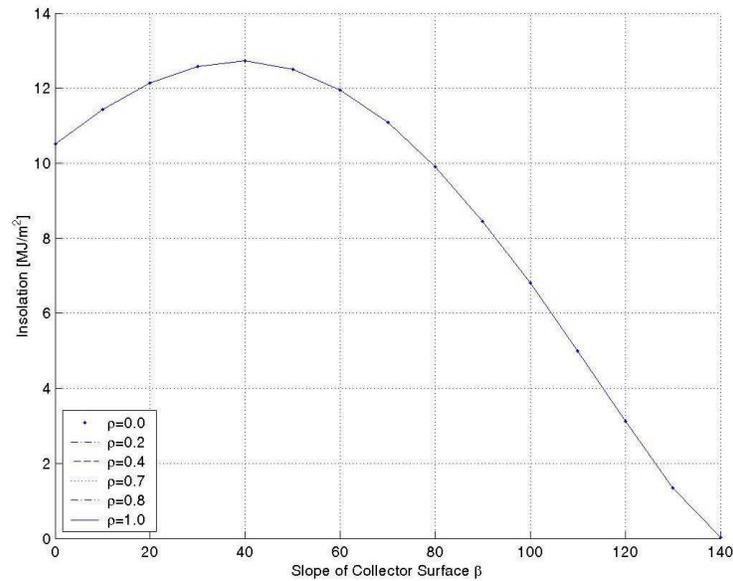

Figure 2.10: Expected daily beam insolation on a tilted surface with different ground reflectivity

Using the Perez et al. (1988) correlation expected average daily totals for each month of the year have been derived at their optimum tilt angles and are presented in table 2.3. As can be seen the seasonal variations are considerable, and surface tilting may increase the available global radiation on average by 37 %. Attention is drawn to the fact that the equations used to calculate these values of *insolation* (in kWh) on tilted surfaces are also valid for determining *radiation* (in kW) at any time during the day. While the Perez et al. (1988) method uses statistical coefficients derived for hourly horizontal insolation measurements (and is therefore not suggested for this purpose) the isotropic correlation suggested by Liu and Jordan (1963) is well suited to the task of determining daily profiles from horizontal data at various surface angles (see figure 2.11 below). The measured data presented in figure 2.11 is part of the dataset recorded by the author.

The data shown in table 2.3 summarises the investigation undertaken in this chapter so far. This data represents the best estimates of radiation that could be attained, and will subsequently also be used to estimate the diesel savings that can be realised by utilising solar-energy devices. As

described above the values have been derived from both the Perez et al. correlation and the average monthly radiation profiles developed at the end of section 2.3.3 in equations 2.5 et al.

Table 2.3: Expected monthly-average daily totals of insolation at SANAE IV

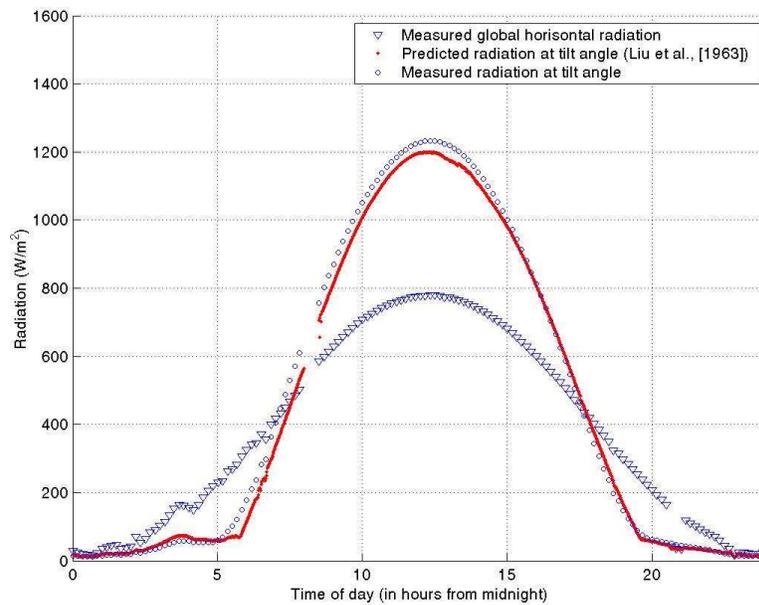| MONTH	GLOBAL HORIZONTAL INSOLATION (kWh/m² day)	OPTIMUM TILT (°) – GLOBAL	TILTED GLOBAL INSOLATION (kWh/m² day)	PERCENTAGE INCREASE AT TILT (%) – GLOBAL	HORIZONTAL BEAM INSOLATION	OPTIMUM TILT (°) – BEAM	TILTED BEAM INSOLATION (kWh/m² day)	PERCENTAGE INCREASE AT TILT (%) – BEAM	AVERAGE TEMP (°C)
Jan	7.26	52	8.05	11	2.92	39	3.54	21	-6.6
Feb	4.78	63	6.11	28	1.88	53	2.99	59	-10.3
Mar	2.13	74	3.51	65	0.74	68	1.99	169	-14.9
Apr	0.72	84	2.54	253	0.26	83	2.12	715	-18.2
May	0.01	90	0.01	0	0.01	90	0.01	0	-19.5
Jun	0.00	00	0.00	0	0.00	00	0.00	0	-20.1
Jul	0.00	00	0.00	0	0.00	00	0.00	0	-23.1
Aug	0.17	88	1.24	629	0.06	87	1.13	1783	-22.9
Sep	1.53	78	3.23	111	0.59	75	2.21	275	-22.9
Oct	3.93	69	6.86	75	1.49	68	3.78	154	-18.2
Nov	6.23	52	7.14	15	2.47	44	3.18	29	-12.8
Dec	7.63	48	8.30	9	3.09	35	3.55	15	-7.1
Avg	*2.87*	*70*	*3.92*	*37*	*1.13*	*64*	*2.04*	*81*	*-16.4*

Figure 2.11: Typical measured and predicted values of radiation for a surface tilted at 40°

Considering figure 2.11, the accuracy of predicting the solar radiation incident on a tilted surface has to be questioned for conditions where the ground is uneven or undulating. Investigation revealed that all predicted daily totals on tilted surfaces derived using the Liu and Jordan isotropic sky method (1963) were on average within 7 % of the actual measured values (that included facing the pyranometer towards hills and snow mounds at various bearings). The largest error was an inaccuracy of 13 %, and all predictions were underestimates. Hence Liu and Jordan (1963) give a reasonable conservative estimate of the expected *radiation* (kW) at various tilt angles for conditions at SANAE IV.

Figure 2.12 gives comparative results of average global horizontal radiation at four Antarctic stations (viz. France's Dumont d'Urville, Sweden's WASA station, Germany's Neumeyer station and South Africa's SANAE IV base) with their respective latitudes indicated in the legend (Henryson et al. [2004], Steel [1993] and Schmidt et al. [1994]). Comparing the estimated radiation with the values suggested for WASA, Dumont d'Urville and Neumeyer it seems that the predicted values of radiation at SANAE IV are reasonable, and an estimate of their accuracy is provided in section 2.4.
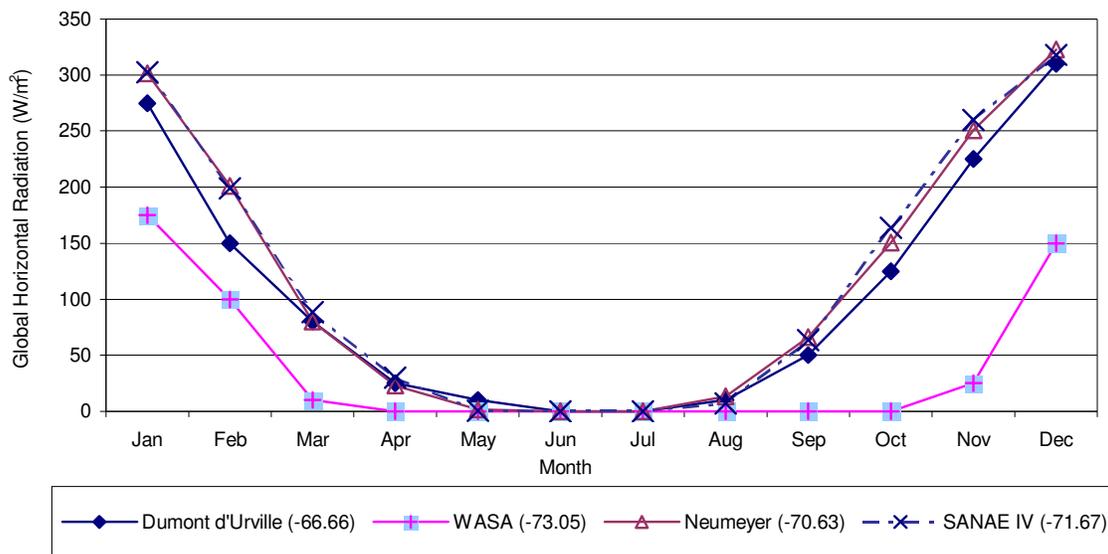

Figure 2.12: Monthly-average global horizontal radiation at four Antarctic stations

2.4 Summary

Available solar energy in Antarctica is characterised, much like many other attributes of the continent, by extremes. During the summer there are exceedingly large amounts of radiation at hand, however, long winter months have the effect of reducing annual averages to such an extent that SANAE IV is classified as a low insolation site.

Estimates of annual insolation have been summarised in table 2.3, and will be used in chapters 4 and 5 to estimate the expected fuel savings from solar energy devices. These values are conservative estimates of the annual radiation at SANAE IV including approximations at the optimal collector tilt angles. As shown in figure 2.12 these radiation values are essentially equal to the conditions at Neumeyer, yet an estimate of the data accuracy for the month of January can be made by noting that actual monthly averages of insolation must be less than clear-sky values. Because it is known that the suggested averages are conservative estimates (c.f. section 2.3.3), and that this data is within 20 % of the clear-sky value (c.f. section 2.3.2), the suggested averages must lie well within 20 % of the actual average. This is especially true considering that only two clear-sky days are expected in January (SSE, 2005).

From table 2.3 it also evident that diffuse radiation forms a significant portion of global radiation (estimated at 1.74 kWh/m^2.day, or 60 % of the average global radiation in table 2.3). Furthermore, figures 2.9 and 2.10 show that collectors will require relatively high tilt angles, starting at 50° in the summer and increasing up to 90° in the winter. This will make it difficult to design compact collector fields since the high tilt angles will not allow placing collectors behind each other.

It is suggested that the potential benefits to the SAWS and BSRN of permanently installing instruments at SANAE IV are investigated. Solar radiation measurements are a fundamental component of any meteorological dataset, significant in view of the fact that although SANAE IV is classified as first class weather station there are currently no instruments at the base measuring solar radiation. This is understandable, however, in view of the associated economic and environmental related difficulties. Measurements of solar radiation at SANAE IV would allow meaningful contributions to be made towards global research projects such as the BSRN.

Chapter 3 – SANAE IV Energy Demand

3.1 Introduction

Diesel is bunkered at SANAE IV in a raised structure located approximately 400 meters from the station. Designed to stockpile almost two year's worth of fuel at once (viz. 600 000 litres) diesel from this bunker is used only for the purposes of refuelling vehicles and supplying the day-tank located in the base. The day-tank in turn supplies diesel to three diesel-electric generators, and these convert the fuel into the two entities of electricity and heat. Together, electricity and heat can be used to classify every single energy load at SANAE IV.

In this chapter the station's energy systems are audited in order to establish which loads are suitable for use with solar electric and solar thermal devices. Utilising these renewable energy devices would be desirable not only for reducing diesel consumption but also for providing the station with greater energy autonomy. Currently 100 % of the electrical and thermal load at the base is met by diesel. Annual diesel demand at SANAE IV amounts to approximately 347 222 litres, of which 297 872 litres are used by the generators for generating electricity, and the remainder is used for re-fuelling the fleet of diesel-powered vehicles. Small amounts of petrol and jet-fuel are also required to power Skidoos and aircraft respectively, yet amount to approximately only 5 % of the overall fuel consumption at the station. Along with diesel the small amounts of petrol and jet-fuel (and negligible amounts of Liquid Petroleum Gas [LPG]) define the complete array of fuels currently utilised at SANAE IV.

There is no obvious replacement for diesel in Antarctica. Internal combustion engines are reliable, safe and easily maintained, used in spite of the difficulties involved with getting fuel to the continent. Heat created by the generators while making electricity is recovered to warm the base and internal combustion engines display an affinity to the cold ambient conditions of Antarctica. It is not surprising that so much time, energy and money are spent on maintaining the current operating systems. Moreover, important machinery such as the diesel-powered vehicles are indispensable to SANAP, and will always require the current diesel infrastructure. It is important to appreciate, however, that on this scale small savings can make a large difference. This is especially true since 81 % of all fuel consumed at SANAE IV is used to generate electricity and heat for the station, two entities very easily displaced by solar alternatives.

3.2 Base Operating Systems

In this chapter a basic layout of the operating systems at SANAE IV is first presented, aimed at providing background to the discussions that follow. Next, quantitative as well as qualitative analyses are undertaken in an attempt to find values of "how much" and "at what times" energy is demanded. This identification of temporal load patterns is particularly important for load-matching renewable resources. Although illustrations that aid in understanding the text have been provided the reader is also directed to appendix C for more information, in which all data presented was collected at the station during the 2004/2005 SANAE IV takeover.

Both Cencelli (2002) and Teetz (2000, 2002) have given descriptions of the SANAE IV station operating systems. Cencelli has mainly classified and explained in some detail how each system operates while Teetz was most interested in quantifying loads. Essentially this chapter draws on their work and is meant to include the changes that have taken place at South Africa's station since their reports were published.

3.2.1 SANAE's Five-fold Operating System

For the purposes of auditing the energy systems at SANAE IV the structure suggested by Cencelli (2002) has been followed. Therefore, all machinery at the station will be classified under one of the following five categories. These are:

1. The Water System,
2. The Heating and Ventilation System,
3. The Power Generation and Electricity Transmission System,
4. The Control or PLC System, and
5. The Sewage System.

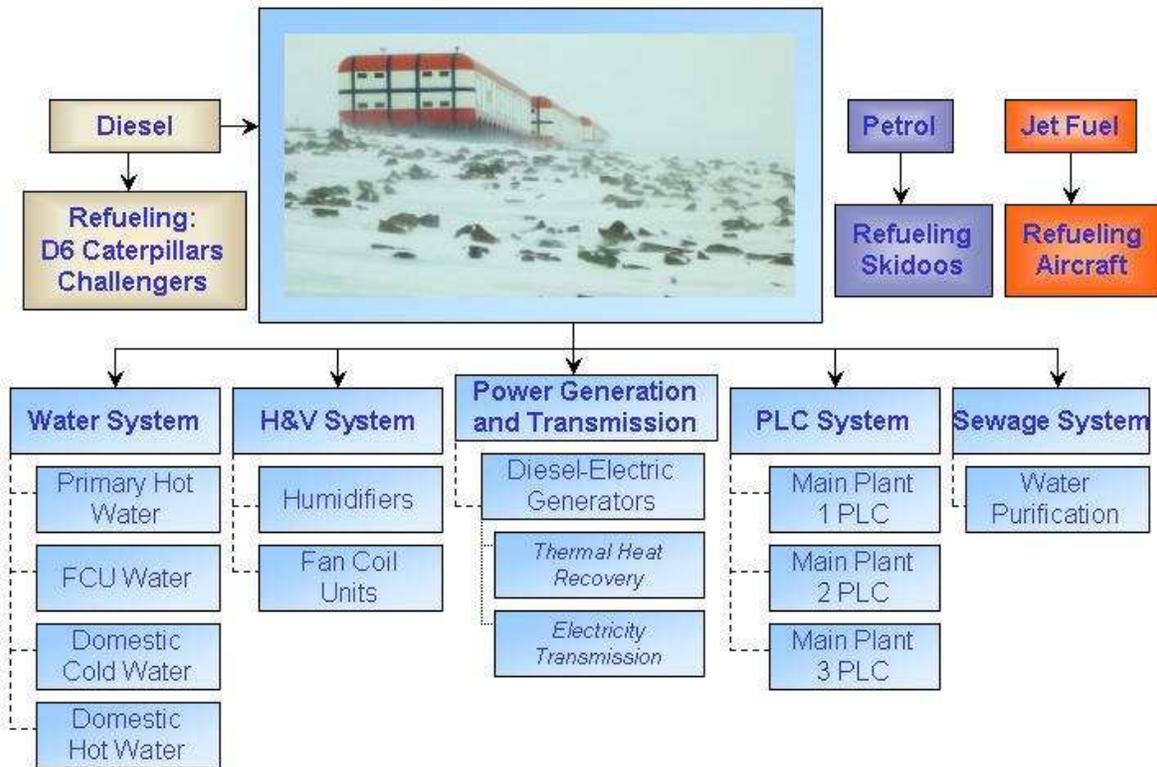Refer to figure 3.1 for an illustration of the above classification system.

Figure 3.1: Energy systems at SANAE IV use only electricity and generator waste heat

3.2.2 Water Systems

Apart from its more obvious properties water is also very useful as an energy transporter. Consequently, the water systems at SANAE IV are responsible not only for supplying the domestic needs of the base (drinking, cooking, cleaning, etc.) but also for transporting heat.

The Primary Hot Water System (refer to figure 3.1) exists as a closed loop within the confines of the plant room. This system is responsible for transporting waste heat from the diesel-electric generators (obtained from the generator coolant fluid as well as the exhaust gasses) to the Fan Coil Unit Water (FCU Water) and Domestic Hot Water Systems and supplements their thermal loads. Typically this method of waste-heat recovery results in exceptional engine efficiencies in the order of around 70 %. Unfortunately, even though the electrical efficiencies of the generators are known (36.4 %, refer to section 3.2.4), the combined or total efficiency cannot currently be calculated. Knowing the inlet and outlet temperatures of the air-conditioning heat exchangers in each block alone (that are recorded daily) is insufficient information to determine this value since the energy transferred at these units includes a significant contribution from inline heating elements that are not recorded. It would be possible to use the temperature difference across the

Primary Hot Water heat exchanger and estimate a flow rate, losses and efficiencies between this heat exchanger and the loads, unfortunately the temperature difference across the Primary Hot Water System is not currently being recorded either.

Next the FCU Water System transports the energy to FCUs located in each block (refer again to figure 3.1). These FCUs in turn heat the outside air (utilising 100 % fresh air with no re-circulation) in order to keep inside temperatures of the base at comfortable levels. The waste-heat recovered from the generators therefore replaces heat lost from the base, which total about 39 kW in summer and 72 kW in winter (Cencelli, 2002).

There are, however, a number of heat sources within the base (computers, lights, people, etc.) that require consideration. Net summer and winter losses (the losses to the environment noted above minus heat given off from internal sources) have been estimated as –10.75 kW (a net heat gain) and 28.5 kW (a net heat loss) respectively, and imply that during summer the station requires cooling. Therefore there is a mismatch between the space-heating demands of the base and the available solar energy throughout the year. Furthermore, this observation begins to explain why summer takeover months are characterised by generator overheating. Since the station requires cooling during summer months the FCU Water Loop cannot use and will not accept generator waste heat. Since the heat-dump designed for these situations is undersized (Cencelli, 2002) heat is trapped inside the Primary Hot Water Loop. As a result the generators begin overheating. A solution sometimes employed by the Engineers is to force the generator heat into the FCU Water Loop (requires overriding normal automatic control), and mix it with more cold outside air by running the FCU fans at higher speeds.

The remaining two water systems, the Domestic Hot and Cold Water (refer to figure 3.1), supply the domestic water needs of the base occupants for cooking, cleaning and sanitation. The demand for fresh water at SANAE IV during the summer takeover period is, however, a source of much distress due to an insufficient water supply from the snow smelter. The snow smelter, a solar thermal and/or solar electrical load is critically important to station functionality, and presents an immediate opportunity for employing solar energy devices.

Lastly, all the water systems operational at SANAE IV are supplemented with water from the twelve storage tanks located along both sides of the hangar in the C-Block. These tanks are capable of storing up to 46 000 litres at a time with the option of isolating tanks from each other.

In this way water can be held in reserve to ensure that a small amount will always be available for keeping the Water Systems operational. There are also a number of unmentioned pumps, controls and in-line heaters associated with these systems that consume energy, and although it is not necessary for the purposes of this discussion to present all detail a more thorough description of each of these systems is provided by Cencelli (2002).

SNOW SMELTER

Antarctica is home to approximately seventy-percent of all the world's fresh water. This reserve, in the form of snow and ice, is consequently also the source of water for the base. In its original form of snow it is of little use, yet the snow smelter (one of biggest energy consumers at the station [refer to figure 3.3]) is able to melt the snow into its liquid form. It is situated approximately 200 meters from the base and is filled by shovelling snow into a chute that leads to one of the two storage tanks located below ground level, known as the "cold" side (refer to figure 3.2). Heating elements within the tanks melt the snow and heat the water while a circulation pump circulates the fluid between the two tanks. Eventually the main pump will pump the water up to the base and into the storage tanks located in the hangar. Together the smelter's two tanks can store 4 600 litres of water though only about half of this volume is normally produced during each smelting session (mainly because of the difficulties involved in compressing the snow as one shovels it into the tank). As a rule there are three snow smelter filling sessions per day during the takeover season.
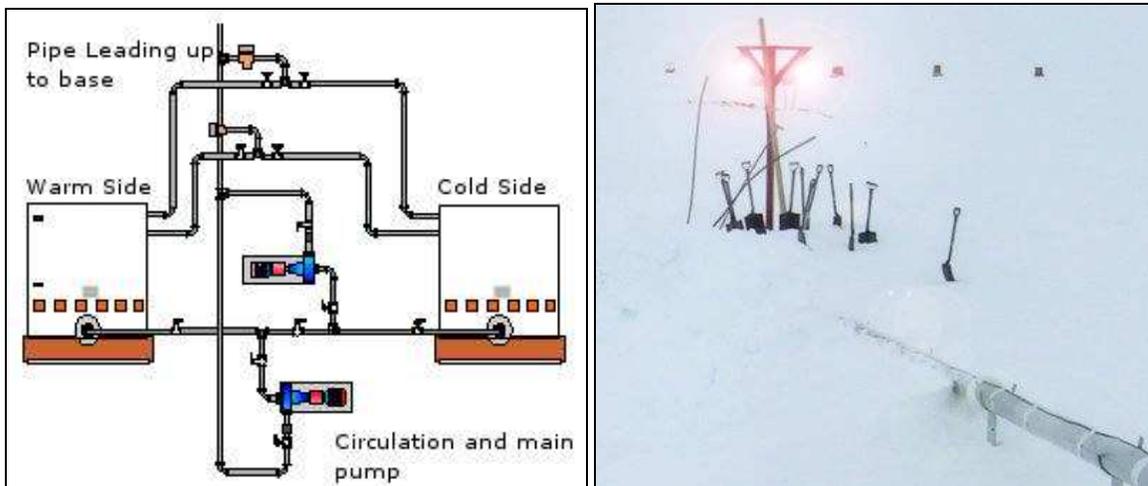

Figure 3.2: The snow smelter (SANAE IV database, 2005)